nature materials

ARTICLES

PUBLISHED ONLINE: 10 NOVEMBER 2013 | DOI: 10.1038/NMAT3783

Observation of unconventional edge states in 'photonic graphene'

Yonatan Plotnik[1†], Mikael C. Rechtsman[1†], Daohong Song[2†], Matthias Heinrich[3], Julia M. Zeuner[3], Stefan Nolte[3], Yaakov Lumer[1], Natalia Malkova[4], Jingjun Xu[2], Alexander Szameit[3], Zhigang Chen[2,4] and Mordechai Segev[1*]

Graphene, a two-dimensional honeycomb lattice of carbon atoms, has been attracting much interest in recent years. Electrons therein behave as massless relativistic particles, giving rise to strikingly unconventional phenomena. Graphene edge states are essential for understanding the electronic properties of this material. However, the coarse or impure nature of the graphene edges hampers the ability to directly probe the edge states. Perhaps the best example is given by the edge states on the bearded edge that have never been observed—because such an edge is unstable in graphene. Here, we use the optical equivalent of graphene—a photonic honeycomb lattice—to study the edge states and their properties. We directly image the edge states on both the zigzag and bearded edges of this photonic graphene, measure their dispersion properties, and most importantly, find a new type of edge state: one residing on the bearded edge that has never been predicted or observed. This edge state lies near the Van Hove singularity in the edge band structure and can be classified as a Tamm-like state lacking any surface defect. The mechanism underlying its formation may counterintuitively appear in other crystalline systems.

Photonic graphene, an array of evanescently coupled waveguides arranged in a honeycomb-lattice configuration, is a useful tool for studying graphene physics[1–14] in optics[15–19], even accessing the nonlinear domain[15,20], which is unfeasible in electronic graphene systems. As the paraxial wave equation (describing propagation of light through a waveguide array) is mathematically equivalent to the Schrödinger equation (describing time evolution of electrons), photonic graphene makes it possible to directly observe graphene wave dynamics using classical light waves. Furthermore, photonic lattices offer exquisite control over initial conditions and allow direct observation of the actual wavefunction (including phase), features that are virtually impossible in electronic systems[21,22]. As the structure of the photonic lattice can be designed at will, and is not subject to structural defects or absorbate contamination (as in carbon-based graphene), photonic graphene provides a window into graphene physics not easily accessible otherwise.

In many proposed graphene-based devices, electrical leads will be placed on the edges, and will thus interact with the electronic edge states[23–26]. There are three types of edge in graphene: the zigzag, bearded and armchair edges[27]. The zigzag and bearded edges have a large and nearly degenerate set of edge states, whereas an unflawed armchair edge has none. Thus far, observation of local electronic edge states of graphene has been achieved by scanning-tunnelling microscopy[28,29], but only at the zigzag edge and at defect points of an armchair edge. The bearded edge has been studied only theoretically[2,27,30]. In fact, edge states on the bearded edge have never been observed, owing to the mechanical instability of the dangling carbon–carbon bonds associated with that edge.

Here, we study—theoretically and experimentally—edge states in photonic graphene lattices. We use a coherent laser beam incident on the zigzag and bearded edges as the probe, and find a new type of edge state that has never been observed nor predicted before. We use two different systems to fabricate our photonic graphene samples: a strongly nonlinear photorefractive crystal where the honeycomb photonic lattice is created using the optical induction method[31]; and a honeycomb-lattice waveguide array written into fused silica by the femtosecond direct laser writing technique[32]. In both cases, a cylindrically focused light beam (akin to a quasi-one-dimensional (1D) wave) is used as a probe launched into the sample along the edge. The degree of diffraction broadening in the direction perpendicular to the edge is a measure of edge confinement, giving a direct experimental probe of whether an edge state is present or not. By changing the launch direction of the probe beam, the presence of the edge state can be probed as a function of the Bloch wavevector. As shown below, we make direct observations of the edge states associated with both the bearded and zigzag edges. Furthermore, we reveal the existence of a new, previously unknown, edge state residing on the bearded edge, whose existence is supported by simulations. This new edge state is classified as 'Tamm-like[33]' as opposed to 'Shockley-like[34]' because it is not associated with band crossings. That said, unlike conventional Tamm states, it is not a result of any real defect on the lattice edge. This new edge state cannot be described by a simple tight-binding model. Rather, a more complete model is needed, as presented in the Supplementary Information.

The structure of the honeycomb lattice along the simplest three terminations of the lattice (bearded, zigzag and armchair) is depicted in Fig. 1a. The lattice is bipartite, meaning that it has two lattice sites per unit cell. The equation describing the diffraction of light in photonic graphene is[11]:

$$i\partial_z \psi(x,y,z) = -\frac{1}{2k_0}\nabla^2\psi(x,y,z) - \frac{k_0 \Delta n(x,y)}{n_0}\psi(x,y,z) \equiv H_{\text{continuum}}\psi \quad (1)$$

[1]Technion—Israel Institute of Technology, Technion City 32000, Haifa, Israel, [2]The MOE Key Laboratory of Weak-Light Nonlinear Photonics, TEDA Applied Physical School and School of Physics, Nankai University, Tianjin 300457, China, [3]Institute of Applied Physics, Friedrich-Schiller-Universität Jena, Max-Wien-Platz 1, 07743 Jena, Germany, [4]Department of Physics and Astronomy, San Francisco State University, San Francisco, California 94132, USA. [†]These authors contributed equally to this work. *e-mail: msegev@technunix.technion.ac.il

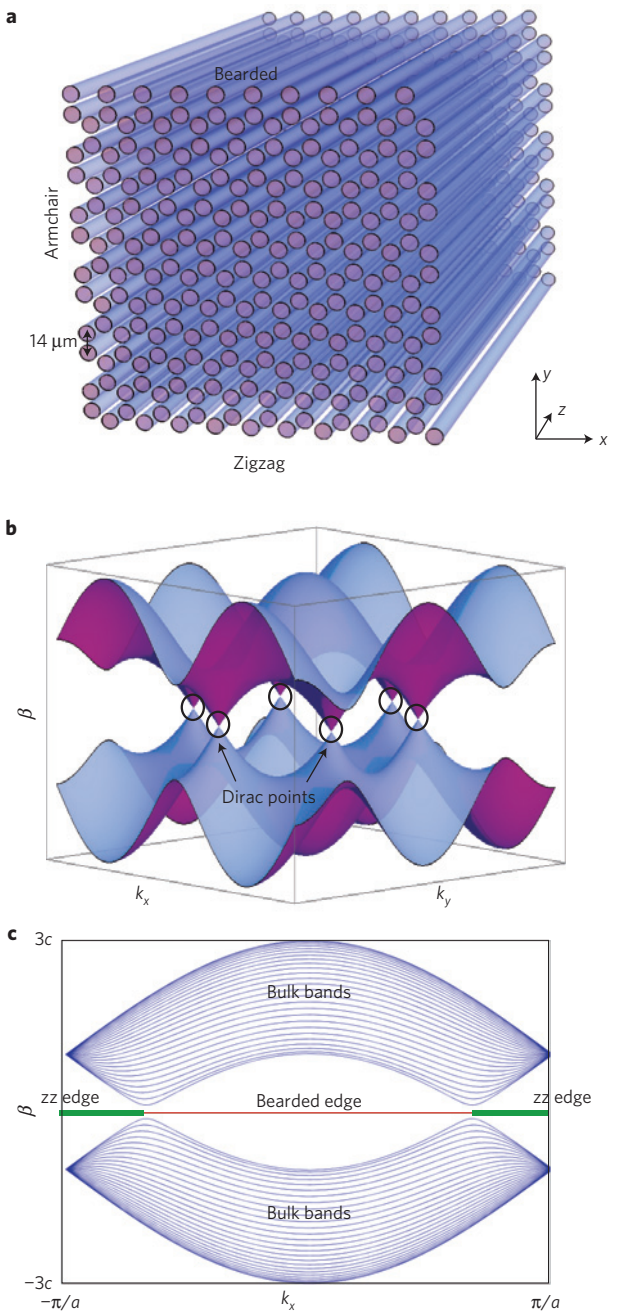

Figure 1 | Physical structure and band structure of photonic honeycomb lattices. a, Schematic image of a honeycomb photonic lattice (array of waveguides), with the three principal edge terminations thereof: bearded, zigzag and armchair edges. **b**, Bulk band structure of photonic graphene, namely propagation constant (β) versus transverse Bloch wavevector, in the nearest-neighbour-coupling tight-binding limit, in units of the nearest-neighbour coupling constant, c, exhibiting Dirac points at the Brillouin zone corners. **c**, Edge band structure of photonic graphene in the same limit. The bulk bands (blue) are eigenstates projected (from **b**) into the edge band structure, whereas the states residing on the bearded and zigzag (zz) edges (red and green, respectively) are intrinsic to the edges.

where z is the longitudinal propagation distance into the photonic lattice; ψ is the envelope of the electric field, defined by $E(x,y,z) = \psi(x,y,z)e^{i(k_0 z-\omega t)}\hat{x}$ (E is the electric field, k_0 is the wavenumber within the medium, $\omega = ck_0/n_0$ and c is the speed of light in vacuum); $\Delta n(x,y)$ is the refractive index structure defining the photonic lattice, and n_0 is the refractive index of the ambient medium in which the lattice is embedded; ∇^2 is the Laplacian in the transverse (x,y) plane; $H_{\text{continuum}}$ as defined in equation (1) is the continuum Hamiltonian for wave propagation in the photonic lattice. Specifics of the refractive index profile, as well as all parameters listed above, are given below and in the Supplementary Information for both the photorefractive and the femtosecond-laser-written systems. The refractive index structure is composed of highly confined waveguides ('potential wells'), each with a single bound state; hence, we employ the 'tight-binding approximation.' In this approximation, the diffraction of light is governed by

$$i\partial_z \psi_n(z) = \sum_j H^{\text{TB}}_{nj}\psi_j(z) \qquad (2)$$

where $\psi_n(z)$ is the amplitude of the nth waveguide mode as a function of z, and H^{TB} is the tight-binding Hamiltonian. In the simplest case, H^{TB} includes only tunnelling between nearest-neighbour waveguides; hence,

$$\sum_j H^{\text{TB}}_{nj}\psi_j = \sum_j c_{nj}\psi_j \qquad (3)$$

where c_{nj} is non-zero only when the nth and jth waveguide are nearest neighbours. This approximation works well to predict the edge states of the Shockley kind, but fails to explain the newly discovered edge modes on the bearded edge. As shown below, a modified tight-binding model with a more complete approximation is needed to explain the existence of these new modes.

Perhaps the best starting point to understand light propagation in photonic lattices is to calculate the band structure of the infinite system with no edges[35]: the eigenvalues (called propagation constants, henceforth labelled β) of the system versus the Bloch wavevector (k_x, k_y; refs 31,35,36). The eigenvalue equation is derived by replacing $\psi(x,y,z)$ in equation (1) with $\psi(x,y)e^{i\beta z}$. The bulk band structure of the honeycomb photonic lattice (with only nearest-neighbour coupling) is plotted in Fig. 1b; the band structure exhibits Dirac points (conical band crossings) characteristic of graphene[2]. Similarly, we plot the band structures for the bearded and zigzag edges (Fig. 1c), assuming nearest-neighbour coupling in the tight-binding model of equation (3). To do that, we find the eigenvalues for a system that is infinite in the x-direction but with bearded and zigzag edges in the y-direction (resulting in a band structure that is a function of only k_x). According to this model, a bearded edge state exists between $k_x = -2\pi/3a$ and $k_x = 2\pi/3a$, and a zigzag edge state exists when the wavevector is outside that range, extending all the way to the boundary of the Brillouin zone (a is the lattice period). Note that, in the nearest-neighbour tight-binding limit (equation (3)), both the bearded and zigzag edge states are entirely dispersionless (the bands are flat)[27]. Earlier experimental work on the graphene electronic edge states has focused on the zigzag case[23,25,28,29], but the state on the bearded edge was never explored experimentally. Using photonic graphene, we can readily investigate both the zigzag and bearded edges, and we find experimentally (supported by simulations) the existence of a new edge state on the bearded edge. As explained below, a refinement of the tight-binding approximations is required to explain it.

We now study the edge states in our first experimental system—an optically induced honeycomb lattice with zigzag and armchair edges (Fig. 2a) in a photorefractive crystal. Here, the photorefractive index change associated with the lattice is about 1.5×10^{-4}, and the lattice constant is 20 μm. A detailed description of the experimental set-up is given in the Supplementary Information. Typical experimental results are shown in Fig. 2. The bright spots in Fig. 2a are the lattice-inducing beams creating the lattice, whereas the higher-index regions are indicated by blue spots. The top and bottom edges are terminated in the zigzag configuration, whereas

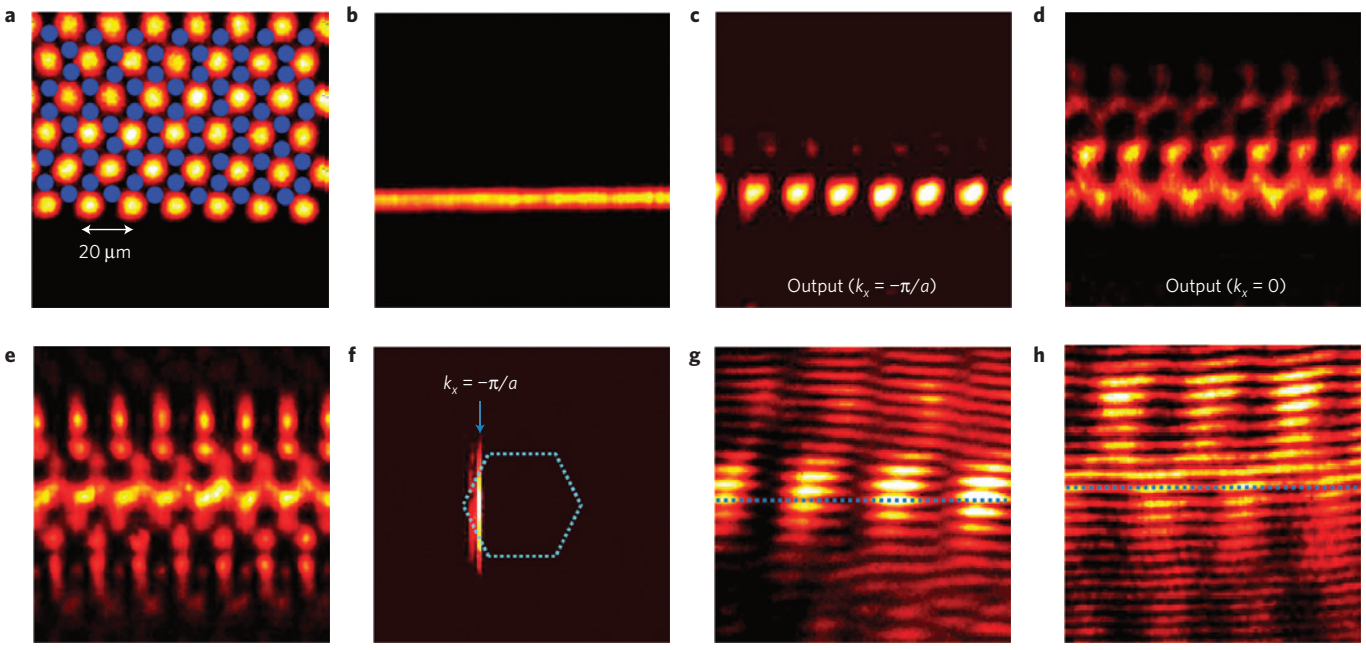

Figure 2 | Experimental demonstration of an edge state at the zigzag edge of an optically induced honeycomb lattice. a, Lattice-inducing beam (bright spots) and corresponding lattice sites (blue spots) induced under self-defocusing photorefractive nonlinearity. **b**, Transverse pattern of an input probe beam launched along the bottom edge in **a**. **c**, Localized output when the input beam is tilted at $k_x = -\pi/a$. **d**, Diffracted output when the input beam is not tilted ($k_x = 0$). **e**, Diffracted output when the input beam is launched straight into the bulk. **f**, Fourier spectrum of the input beam corresponding to **c**. **g**,**h**, Interferograms of output (**c**,**d**) with a tilted broad beam showing the staggered phase (**g**) and the uniform phase (**h**) of the output field along the edge. Note that **c** and **f** have been lightened to improve visibility.

the left and right edges in the armchair configuration. When a stripe beam is sent as a probe along the armchair surface, we observe no edge state: the beam experiences diffraction broadening in the direction perpendicular to the edge. However, when the stripe beam is used to probe the zigzag edge, we observe formation of an edge state under appropriate launch conditions. Specifically, when the input probe beam (Fig. 2b) enters at an angle that corresponds to a wavevector close to $k_x = -\pi/a$, strong surface confinement is observed at the output of the photonic lattice (Fig. 2c). In contrast, when the probe beam is launched at normal incidence into the lattice such that $k_x = 0$, no surface confinement is observed; rather, the beam diffracts away from the edge into the bulk of the lattice (Fig. 2d). For comparison, it is instructive to examine the symmetric diffraction of the probe beam when launched into the bulk of the lattice, as shown in Fig. 2e. Comparing the Fourier spectrum of the input beam with the lattice Brillouin zone (marked by blue dashed lines; Fig. 2f), we see that the input beam indeed excites the spectral region in which the zigzag edge state resides, that is, near the boundary of the edge Brillouin zone at $k_x = -\pi/a$ (Fig. 1c). The difference between excitations at $k_x = -\pi/a$ and $k_x = 0$ can also be seen from the measurement of phase gradient, simply by interfering the output beams in Fig. 2c,d with a tilted plane wave. Such interferograms are as shown in Fig. 2g,h. The interference fringes at $k_x = -\pi/a$ interleave—exhibiting a minimum between consecutive peaks (Fig. 2g), indicating a staggered phase structure along the horizontal direction, whereas at $k_x = 0$ the phase is uniform (Fig. 2h). The light confinement at the zigzag edge at $k_x = -\pi/a$ with the staggered phase indicates the presence of the edge state, whereas in the bulk the same launch beam experiences diffractive broadening. This proves the experimental observation of the edge state residing at the zigzag edge.

Next, we test the prediction shown in Fig. 1c: that the zigzag edge states exist only for $|k_x| \geq 2\pi/3a$. Such experiments are more readily testable in our second experimental system: the femtosecond-laser-written samples in fused silica, where edges can easily be made abrupt. In the experimental set-up, described in the Supplementary Information, a HeNe laser beam is shaped and launched on the input face of the photonic lattice in a variety of horizontal angles related to different k_x. Figure 3a shows a microscope image of the input facet of the honeycomb photonic lattice with a bearded edge at the top and a zigzag edge at the bottom. The waveguides are elliptical (horizontal and vertical diameters of 11 and 4 μm, respectively), and have nearest-neighbour spacing of 14 μm. The functional form of a single waveguide is given by $\Delta n(x,y) = 7 \times 10^{-4} e^{-((2x/d_1)^2+(2y/d_2)^2)^3}$. The ellipticity leads to some anisotropy in the inter-waveguide coupling but it is small and can be ignored. The red ovals in the figure indicate the structure of the input light: an elliptical beam with its long axis running along the edge. Thus, we probe the entire edge Brillouin zone by varying the input angle of the beam; this introduces a linear phase gradient parallel to the edge and therefore selects a particular Bloch wavevector, k_x. If at a given k_x, light is confined to the edge on which it was incident, then an edge state exists, and otherwise it does not. The beam is sufficiently wide along the edge so that it is narrow in k_x-space and thus probes near a particular k_x.

The light emerging from the output facet of the honeycomb sample is shown for the four cases: when the input beam is incident on the zigzag edge, with incident angle such that $k_x = 0$ (Fig. 3b); the zigzag edge, with $k_x = \pi/a$ (Fig. 3c); the bearded edge with $k_x = 0$ (Fig. 3d); and the bearded edge with $k_x = \pi/a$ (Fig. 3e). In the first case of Fig. 3b, light is not confined to the zigzag edge but instead diffracts into the bulk. This is consistent with results obtained in our first experimental system (Fig. 2d). As for the results in Fig. 2c, near $k_x = \pi/a$ light stays confined to the edge owing to the presence of an edge state. On the bearded edge, the existence of the edge state at $k_x = 0$ is evident in Fig. 3d where light is confined on the edge. This constitutes the first experimental observation of an edge state on the bearded edge of a honeycomb lattice,

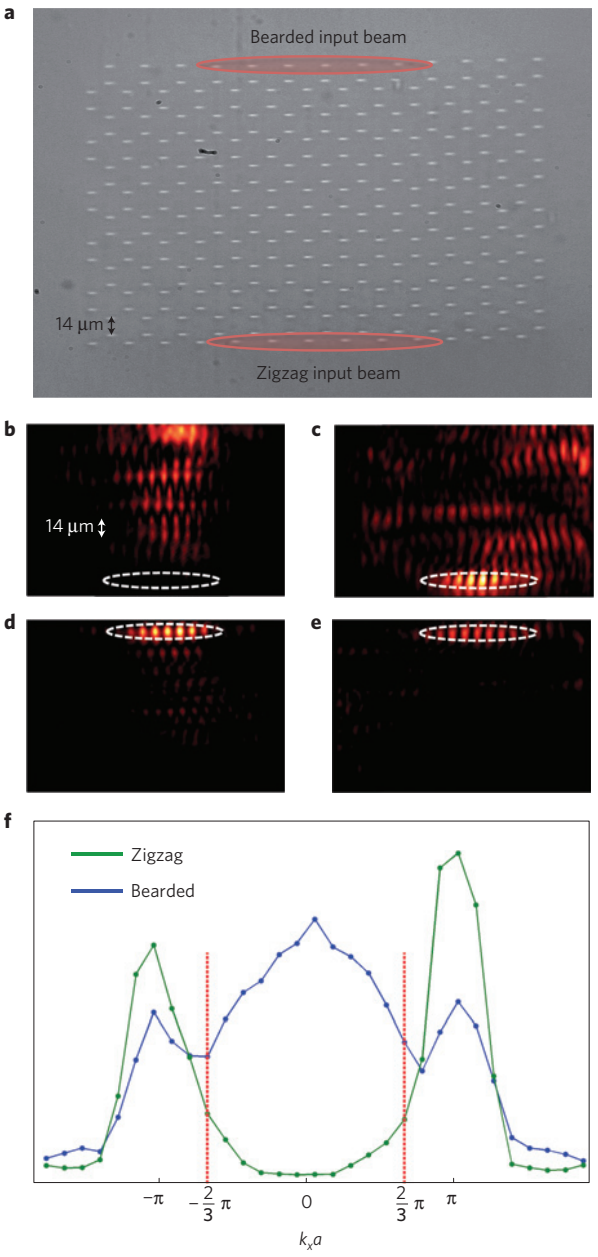

Figure 3 | Momentum-resolved measurements of edge states in a photonic honeycomb lattice. a, Microscope image of the input facet of a femtosecond-written honeycomb lattice. Red ellipses mark the input beams for the bearded and zigzag edges. **b**–**e**, Wavefunction emerging from the output facets for: probe beam launched at zigzag edge at $k = 0$, leading to diffraction into the bulk (**b**), probe launched at zigzag edge at $k = \pi/a$ leading to edge confinement due to the presence of an edge state (**c**), probe launched at bearded edge at $k = 0$ leading to confinement due to the presence of the standard bearded edge state (**d**), probe launched at bearded edge at $k = \pi/a$ (**e**), exhibiting edge confinement due to the newly observed edge state. Dashed ellipses mark the expected position of the output beam when an edge state is present. **f**, Fraction of power confined to the edge for the zigzag (green) and bearded (blue) edges; the peaks indicate strong confinement due to the presence of edge states. Note that **b**–**e** have been lightened to improve visibility.

which was predicted[30] but never observed. However, perhaps the most important observation of this work is shown in Fig. 3e: near $k_x = \pi/a$, light remains confined to the bearded edge despite the fact that edge states have not been previously predicted for this Bloch wavevector on the bearded edge in a system without defects[27,30]. We plot the fraction of optical power that remains confined on the edge of the structure in Fig. 3f, where the edge is defined as the two outer rows of waveguides. For the zigzag edge, the results are as predicted by the simple tight-binding model: for a large range of k_x for which there is no zigzag edge state ($k_x = -2\pi/3a$ through $k_x = 2\pi/3a$), the light largely diffracts into the bulk. However, outside this region, most of the light remains on the edge. For the bearded edge, on the other hand, the results differ significantly from what is predicted by simple tight-binding theory. Indeed, light is highly confined on the edge within the range of the bearded edge state ($k_x = -2\pi/3a$ through $k_x = 2\pi/3a$), as predicted, but Fig. 3c clearly shows that light remains confined also outside this region, reaching local maxima at $k_x = \pm\pi/a$. Thus, our experiments have provided evidence for a new state residing on the bearded edge. Obviously, this experimental finding calls for an explanation. As we discuss below, the existence of this new edge state is supported by the full continuum description of the honeycomb lattice (equation (1)), but it does not arise from the commonly used tight-binding model (equations (2) and (3)), as the other, previously known, edge states of the graphene structure do. A refinement of the tight-binding approximations is needed to account for the new edge state.

The presence of the new edge state on the bearded edge and its band structure (Fig. 4a) are revealed by a full-continuum calculation (that is, by diagonalizing equation (1)). The refractive index structure of the unit cell used for the calculation is shown in Fig. 4b. The absolute value of a bulk eigenfunction $\psi(x, y)$ is shown in Fig. 4c: it is the eigenfunction associated with the largest propagation constant, β, at $k_x = 0$. In the continuum model, the bearded and zigzag edge states no longer have flat bands associated with them (as the nearest-neighbour tight-binding model predicts), but rather now have some weak dispersion associated with the curvature of the edge bands. This can be seen by comparing Fig. 4a with Fig. 1c. The standard bearded edge states are shown at $k_x = 0$ and standard zigzag edge states are shown at $k_x = \pi/a$, in Fig. 4d,e respectively. Importantly, the continuum band structure contains two new edge states associated with the bearded edge, which emerge at the boundaries of the edge Brillouin zone (the two sides of Fig. 4a), and are shown in Fig. 4f,g. These edge states are more extended into the bulk than the other edge states, and they lie extremely close to the bulk bands (again in contrast to the other edge states). In addition, in contrast to the known edge states occupying only one of the sublattices, these new edge states occupy both sublattices. This is shown in detail in Fig. 4h, which is simply a zoomed-in plot of Fig. 4a, at the boundaries of the edge Brillouin zone. Note that the band structure is periodic, and thus it repeats with period $2\pi/a$.

These new edge states may be classified as 'Tamm states'[33] (as opposed to 'Shockley states'[34]), because they do not arise from a band crossing, the criterion for the emergence of Shockley states[37]. That said, Tamm states are conventionally associated with surface perturbations or defects (that are inherent in the system, or that arise from modulation[38,39]), although, in the present case no defects whatsoever are present. What happens here is that the edge itself acts as a sufficiently strong defect to localize light on the edge. This effect, which cannot be accounted for in standard tight-binding theory, is described below and in more detail in the Supplementary Information. The observation of these edge states associated with the bearded edge in the continuum simulations shown in Fig. 4 accounts for the strong confinement on the bearded edge at the Brillouin zone boundary, as shown in Fig. 3c.

To explain the newly discovered edge states in the context of the tight-binding model, one must account for additional terms. Namely, the on-site propagation constant of each mode is modified by the refractive index of its neighbouring sites. This modification differentiates between bulk sites, which have three neighbours,

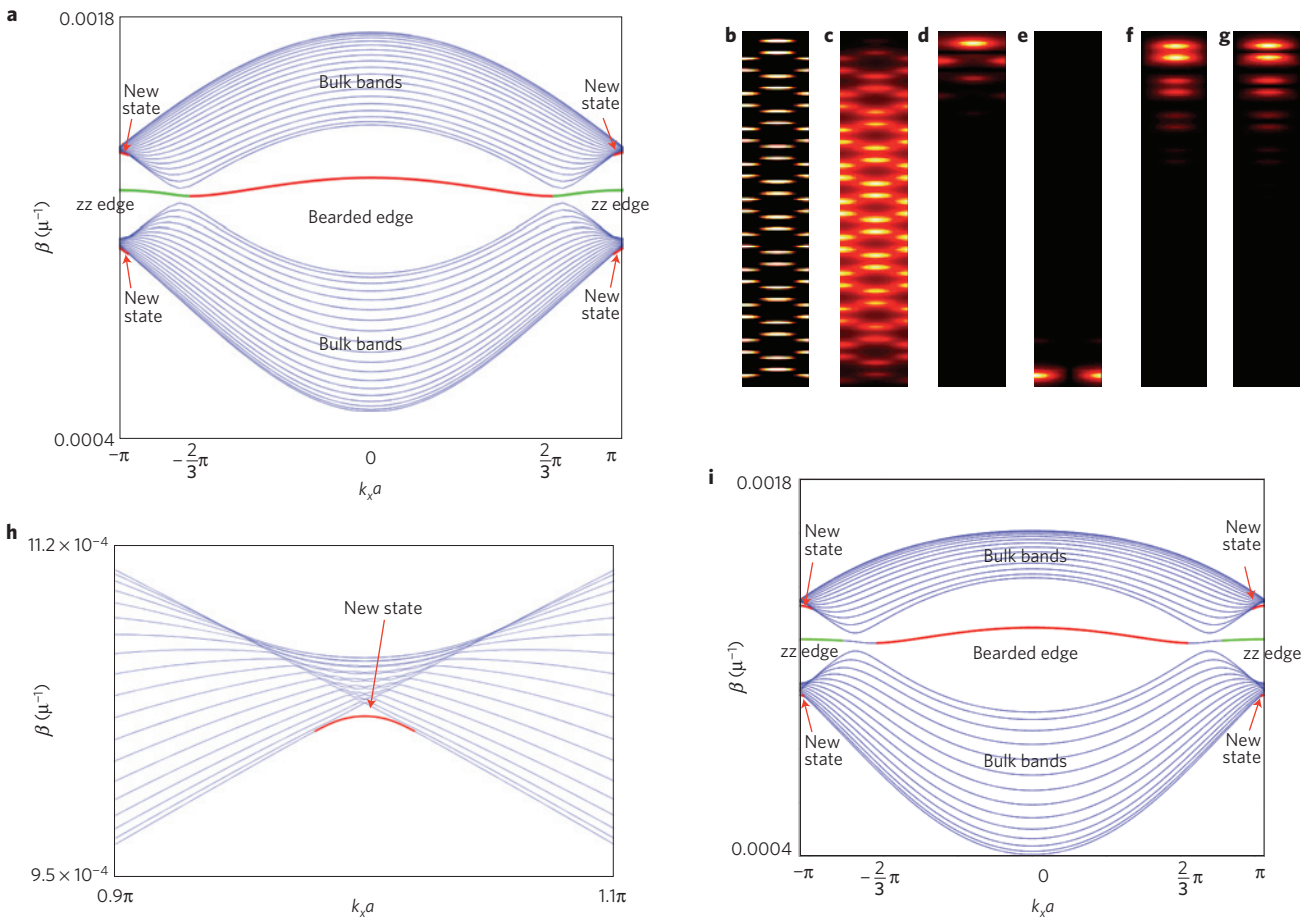

Figure 4 | Calculating the new edge state. a, Edge band structure calculated using the full continuum description (equation (1)). The calculation reveals the zigzag and bearded edge states known from the nearest-neighbour tight-binding description (Fig. 1c), but two more edge states appear on the bearded edge, at the edge Brillouin zone boundary. **b**, Refractive index structure used to calculate the edge band containing the bearded (top) and zigzag (bottom) edges. The cell dimensions are $24 \times 420\ \mu m^2$. **c**, Bulk ground state at $k = 0$. **d**, Bearded edge state at $k = 0$. **e**, Zigzag edge state at $k = \pi/a$. **f**, The new bearded edge state at $k = \pi/a$ (top band). **g**, The new bearded edge state at $k = \pi/a$ (bottom band). **h**, The same as in **a**, zoom in on the Brillouin-zone edge in the top band. **i**, Similar to **a**, but using the modified tight-binding model incorporating modified on-site energy. The clear agreement between **a** and **i** proves the validity of the model in predicting the new edge states.

and bearded edge sites, which have only one neighbour. This difference is small and can be neglected to first order, but comes into play where the modes are highly degenerate, as in the Van Hove singularity at the edge of the Brillouin zone. At the degeneracy point, any slight edge perturbation takes the edge mode out of the band and creates a Tamm-like edge state as shown in Fig. 4i. We emphasize again that this Tamm-like state does not result from any real surface perturbation but rather the specific surface structure along the bearded edge. Note that the effect is stronger on the bearded edge, compared with the zigzag edge, because the waveguides on the former are 'missing' two bonds, whereas those on the latter are missing only one. This explanation is elaborated further in the Supplementary Information, where we also explain why the edge state appears at exactly $k_x = \pi/a$.

In conclusion, studying systems analogous to carbon-based graphene (as in this work) provides a window into new graphene physics that may otherwise remain unobserved or elusive owing to structural disorder, mechanical instabilities, and the sheer difficulty of obtaining large and pure graphene nanoribbons. Our experiments show that the observation of the richness of graphene physics does not need to be constrained by present-day fabrication and chemical isolation limitations. The detailed understanding of edge states is essential not just for transport properties, as surface science in general has produced a large variety of new physics that cannot be found when examining just the material bulk. Indeed, edge states play a signature role in electron dynamics in the quantum Hall effect and both 2D and 3D topological insulators. The important goal of realizing a robust optical topological insulator relies on the understanding of photonic edge states. Owing to its exquisite tunability, the waveguide array system described here provides an ideal platform for achieving this goal[40].

The class of edge states discussed here is distinct from standard graphene edge states in a number of ways, and thus yields unexpected edge physics. Specifically, unlike previously known states, they are not captured in standard tight-binding models, and they cannot be derived from Zak phase arguments[41]; they are highly dispersive and non-flat (very small effective mass). Furthermore, there are two of these new edge states at a given k_x, and when both are excited, they exhibit beating (periodic oscillations). Finally, they reside on both sublattices of the honeycomb unit cell, contrary to the previously known edge states, which reside only on one sub-lattice. These distinctions call forward the questions of whether such states can be observed in graphene itself, what effect they may have on electronic transport, and not least, whether they can be topologically protected under the influence of time-reversal symmetry breaking.

In this work, we have studied the existence of edge states in a honeycomb photonic lattice. While observing edge states that were previously predicted, we discovered new edge states that involve interesting new physics. Our investigation and explanation of the new edge state raises an interesting point: this type of defect-free Tamm state is likely to appear in other systems beyond graphene. Clearly, the crucial feature for the appearance of such a state is a point of high degeneracy in the band structure. It is therefore likely that such edge states will also appear in kagome lattices and other lattice structures.

Received 30 October 2012; accepted 18 September 2013; published online 10 November 2013

References

1. Novoselov, K. S. *et al.* Two-dimensional gas of massless Dirac fermions in graphene. *Nature* **438,** 197–200 (2005).
2. Castro Neto, A. H., Guinea, F., Peres, N. M. R., Novoselov, K. S. & Geim, A. K. The electronic properties of graphene. *Rev. Mod. Phys.* **81,** 109–162 (2009).
3. Beenakker, C. W. J. Colloquium: Andreev reflection and Klein tunneling in graphene. *Rev. Mod. Phys.* **80,** 1337–1354 (2008).
4. Zhang, Y., Tan, Y-W., Stormer, H. L. & Kim, P. Experimental observation of the quantum Hall effect and Berry's phase in graphene. *Nature* **438,** 201–204 (2005).
5. Guinea, F., Katsnelson, M. I. & Geim, A. K. Energy gaps and a zero-field quantum Hall effect in graphene by strain engineering. *Nature Phys.* **6,** 30–33 (2010).
6. Montambaux, G., Piéchon, F., Fuchs, J-N. & Goerbig, M. O. Merging of Dirac points in a two-dimensional crystal. *Phys. Rev. B* **80,** 153412 (2009).
7. Fefferman, C. & Weinstein, M. Honeycomb lattice potentials and Dirac points. *J. Am. Math. Soc.* **25,** 1169–1220 (2012).
8. Tarruell, L., Greif, D., Uehlinger, T., Jotzu, G. & Esslinger, T. Creating, moving and merging Dirac points with a Fermi gas in a tunable honeycomb lattice. *Nature* **483,** 302–305 (2012).
9. Gomes, K. K., Mar, W., Ko, W., Guinea, F. & Manoharan, H. C. Designer Dirac fermions and topological phases in molecular graphene. *Nature* **483,** 306–310 (2012).
10. Wertz, E. *et al.* Spontaneous formation and optical manipulation of extended polariton condensates. *Nature Phys.* **6,** 860–864 (2010).
11. Goldman, N., Beugnon, J. & Gerbier, F. Detecting chiral edge states in the hofstadter optical lattice. *Phys. Rev. Lett.* **108,** 255303 (2012).
12. Carusotto, I. & Ciuti, C. Quantum fluids of light. *Rev. Mod. Phys.* **85,** 299–366 (2013).
13. Kuhl, U. *et al.* Dirac point and edge states in a microwave realization of tight-binding graphene-like structures. *Phys. Rev. B* **82,** 094308 (2010).
14. Bellec, M., Kuhl, U., Montambaux, G. & Mortessagne, F. Topological transition of Dirac points in a microwave experiment. *Phys. Rev. Lett.* **110,** 033902 (2013).
15. Peleg, O. *et al.* Conical diffraction and gap solitons in honeycomb photonic lattices. *Phys. Rev. Lett.* **98,** 103901 (2007).
16. Sepkhanov, R. A., Bazaliy, Y. B. & Beenakker, C. W. J. Extremal transmission at the Dirac point of a photonic band structure. *Phys. Rev. A* **75,** 063813 (2007).
17. Bahat-Treidel, O., Peleg, O. & Segev, M. Symmetry breaking in honeycomb photonic lattices. *Opt. Lett.* **33,** 2251–2253 (2008).
18. Polini, M., Guinea, F., Lewenstein, M., Manoharan, H. C. & Pellegrini, V. Artificial honeycomb lattices for electrons, atoms and photons. *Nature Nanotech.* **8,** 625–633 (2013).
19. Bahat-Treidel, O. *et al.* Klein tunneling in deformed honeycomb lattices. *Phys. Rev. Lett.* **104,** 063901 (2010).
20. Ablowitz, M. J., Nixon, S. D. & Zhu, Y. Conical diffraction in honeycomb lattices. *Phys. Rev. A* **79,** 053830 (2009).
21. Bartal, G. *et al.* Brillouin zone spectroscopy of nonlinear photonic lattices. *Phys. Rev. Lett.* **94,** 163902 (2005).
22. Eisenberg, H. S., Silberberg, Y., Morandotti, R., Boyd, A. R. & Aitchison, J. S. Discrete spatial optical solitons in waveguide arrays. *Phys. Rev. Lett.* **81,** 3383–3386 (1998).
23. Fujita, M., Wakabayashi, K., Nakada, K. & Kusakabe, K. Peculiar localized state at zigzag graphite edge. *J. Phys. Soc. Jpn* **65,** 1920–1923 (1996).
24. Özyilmaz, B. *et al.* Electronic transport and quantum Hall effect in bipolar graphene p–n–p junctions. *Phys. Rev. Lett.* **99,** 166804 (2007).
25. Ritter, K. A. & Lyding, J. W. The influence of edge structure on the electronic properties of graphene quantum dots and nanoribbons. *Nature Mater.* **8,** 235–242 (2009).
26. Yao, W., Yang, S. A. & Niu, Q. Edge states in graphene: From gapped flat-band to gapless chiral modes. *Phys. Rev. Lett.* **102,** 096801 (2009).
27. Kohmoto, M. & Hasegawa, Y. Zero modes and edge states of the honeycomb lattice. *Phys. Rev. B* **76,** 205402 (2007).
28. Kobayashi, Y., Fukui, K., Enoki, T., Kusakabe, K. & Kaburagi, Y. Observation of zigzag and armchair edges of graphite using scanning tunneling microscopy and spectroscopy. *Phys. Rev. B* **71,** 193406 (2005).
29. Tao, C. *et al.* Spatially resolving edge states of chiral graphene nanoribbons. *Nature Phys.* **7,** 616–620 (2011).
30. Klein, D. J. Graphitic polymer strips with edge states. *Chem. Phys. Lett.* **217,** 261–265 (1994).
31. Efremidis, N. K., Sears, S., Christodoulides, D. N., Fleischer, J. W. & Segev, M. Discrete solitons in photorefractive optically induced photonic lattices. *Phys. Rev. E* **66,** 046602 (2002).
32. Szameit, A. *et al.* Discrete nonlinear localization in femtosecond laser written waveguides in fused silica. *Opt. Express* **13,** 10552–10557 (2005).
33. Tamm, I. E. On the possible bound states of electrons on a crystal surface. *Phys. Z. Sowjetunion* **1,** 733–735 (1932).
34. Shockley, W. On the surface states associated with a periodic potential. *Phys. Rev.* **56,** 317–323 (1939).
35. Lederer, F. *et al.* Discrete solitons in optics. *Phys. Rep.* **463,** 1–126 (2008).
36. Fleischer, J. W., Segev, M., Efremidis, N. K. & Christodoulides, D. N. Observation of two-dimensional discrete solitons in optically induced nonlinear photonic lattices. *Nature* **422,** 147–150 (2003).
37. Malkova, N., Hromada, I., Wang, X., Bryant, G. & Chen, Z. Observation of optical Shockley-like surface states in photonic superlattices. *Opt. Lett.* **34,** 1633–1635 (2009).
38. Garanovich, I. L., Sukhorukov, A. A. & Kivshar, Y. S. Defect free surface state in modulated photonic lattices. *Phys. Rev. Lett.* **100,** 203904 (2008).
39. Szameit, A. *et al.* Observation of defect-free surface modes in optical waveguide arrays. *Phys. Rev. Lett.* **101,** 203902 (2008).
40. Rechtsman, M. C. *et al.* Photonic Floquet topological insulators. *Nature* **496,** 196–200 (2013).
41. Zak, J. Berry's phase for energy bands in solids. *Phys. Rev. Lett.* **62,** 2747–2750 (1989).

Acknowledgements

The Technion team is part of the Israeli Center of Research Excellence 'Circle of Light' supported by the I-CORE Program of the Planning and Budgeting Committee and The Israel Science Foundation. M.C.R. is grateful to the Azrieli foundation for the Azrieli fellowship. This research was financially supported by an Advanced Grant from the European Research Council; the Israel Science Foundation; the USA-Israel Binational Science Foundation; the German Ministry of Education and Science (ZIK 03Z1HN31); the 973 Programs (2013CB328702, 2013CB632703) and the Program for Changjiang Scholars and Innovative Research Teams in China; and by the NSF and AFOSR in the USA.

Author contributions

All authors contributed significantly to this work.

Additional information

Supplementary information is available in the online version of the paper. Reprints and permissions information is available online at www.nature.com/reprints. Correspondence and requests for materials should be addressed to M.S.

Competing financial interests

The authors declare no competing financial interests.